

Hemocompatibility of poly(ether imide) membranes functionalized with carboxylic groups

R. Tzoneva · B. Seifert · W. Albrecht · K. Richau · T. Groth · A. Lendlein

Received: 16 March 2007 / Accepted: 16 April 2008 / Published online: 2 May 2008
© Springer Science+Business Media, LLC 2008

Abstract Materials for blood-contacting applications have to meet high requirements in terms to prevent thrombotic complications after the medical treatment. Surface induced thrombosis, e.g., after application of cardiovascular devices, is linked clearly to the activation of coagulation system and platelet adhesion and activation. The flat sheet poly(ether imide) membrane (PEI) was modified by binding of iminodiacetic acid (IDA) for different periods of time to obtain surfaces with carboxylic (–COOH) groups, namely PEI-1 (modified for 1 min) and PEI-2 (modified for 30 min). The successful binding of the ligands was monitored by thionin acetate assay. The physico-chemical characteristics of the materials were analyzed by SEM, AFM, water contact angle, and Zeta potential measurements. Hemocompatibility of the polymer materials was studied by analyzing the activation of coagulation system (plasma kallikrein-like activity) and platelet adhesion/activation by using immunofluorescence technique. The blood response to PEI membranes was compared to that of a commercial poly(ethylene terephthalate) (PET) membrane. Our results showed that the increase of the negative charges on the modified PEI

membrane surfaces (number of –COOH groups) caused a higher contact activation of the coagulation system and a higher rate of platelet adhesion and activation compared to non-modified PEI. However, overall the hemocompatibility of all PEI membranes was higher than that of PET.

1 Introduction

Thrombosis is a major complication which occurs when a foreign surface contacts blood [1]. One of the strategies to improve hemocompatibility of the material devices is surface modification by adding different functional groups such as hydroxyl (–OH), amine (–NH_x), sulfate (–SO₄), or carboxylic (–COOH) [2, 3]. These functional groups can be utilized in engineering biomedical surfaces to improve the spreading and growth of certain cells [4], and to immobilize biomolecules (enzymes, peptides, etc.) by means of “spacer arm” molecules [5] of a certain length, that keep them tethered at the surface with their biological activity unaltered. A number of investigators have shown that polymers incorporating carboxylic groups have rather remarkable blood-contacting properties. These materials may act like heparin, a mucopolysaccharide, which is used as an anticoagulant. Carboxylic groups together with sulfate groups have been shown to be essential for the anticoagulant activity of heparin [6, 7].

The present research continues our efforts to produce more hemocompatible polymer surfaces, based on PEI membranes. Our approach has been to determine how the surface properties (as surface charge) of PEI affect the key steps during thrombus formation: contact activation and platelet adhesion/activation. Polyimide materials such as PEI are a new advancing class of polymer materials for

R. Tzoneva (✉)
Institute of Biophysics, Bulgarian Academy of Sciences,
Acad. G. Bonchev St., Bl. 108, Sofia 1113, Bulgaria
e-mail: tzoneva@bio21.bas.bg

B. Seifert · W. Albrecht · K. Richau · A. Lendlein
Institute of Polymer Research, GKSS Research Centre,
Kantstrasse 55, 14513 Teltow, Germany

T. Groth
Biomedical Materials Group, Department of Pharmaceutics
and Biopharmaceutics, Institute of Pharmacy, Martin Luther
University, Halle-Wittenberg, Kurt-Mothes-Strasse 1,
06120 Halle (Saale), Germany

biomedical applications [8, 9] and the investigations of their biocompatibility have shown a low immune response and good cell attachment and growth [2, 10–12]. In our previous work [13] we showed that the hydrophobic nature of PEI membrane (advancing contact angle of 78°C) caused a “passivation effect” on the surface in terms of low activation rate of adherent platelets. In addition, the considerable mechanical strength and the thermal stability [14] of PEI make this membrane suitable for steam sterilization. Furthermore, the presence of functional groups on the polymer backbone enhances the membrane-forming properties [15] and enables the resulting membrane to be adapted to the desirable application. In this study, we introduced carboxylic groups on the PEI surface by a heterogeneous functionalization process [16]. The carboxylation of the polymer surfaces was done with the knowledge that –COOH end groups may also be used for subsequent creation of bio-inert, pegylated surfaces [17], and/or for heparinized surfaces [6]. The advantages using this surface modification of the polymer was arising from the fact that heparin substitutes based only on carboxylic acid groups and devoid of sulfate groups might facilitate easy prodrug approach for passage through the gastrointestinal lining [18]. In addition, a recent study of the antithrombin-activating properties of a carboxylic acid-based polymer, poly(acrylic acid), demonstrated a surprisingly high acceleration of thrombin and factor Xa inhibition [19].

Thus the surface modification with –COOH end groups was expected to provide surfaces with improved blood compatibility. Two modified PEI membranes, distinguished by different times of modification process and the number of –COOH groups on the surface, were investigated. The blood compatibility of the membranes was studied *in vitro* by measuring the activation of coagulation system and the adhesion and activation rate of platelets.

2 Materials and methods

2.1 Polymers and membrane modification

Poly(ether imide) (PEI) flat membranes were prepared from a commercial polymer (Ultem[®] 1000, General Electric, New York, USA) by a conventional phase inversion process as described previously [20]. Carboxylic groups on the polymer surface were produced by wet chemistry. The dry flat membrane was contacted with the modifier solution (2 wt% of the sodium salt of iminodiacetic acid (IDA), dissolved in 1:1 mixture of 1-propanol and water) under stirring at 70°C for up to 30 min. After quenching in cool water and intensely rinsing the membranes were stored in wet state at 4°C until use.

2.2 Reference membrane

As reference membrane a poly(ethylene terephthalate) (PET, Oxyphen GmbH, Dresden, Germany) film with the thickness of 23 µm and low porosity was used.

2.3 Scanning electron microscopy (SEM)

The morphology of unmodified PEI and both modified PEI membranes were investigated by SEM. For that purpose, the membranes were fractured in liquid nitrogen and coated with gold/palladium (8/20) under vacuum. The prepared samples were studied in a JSM 6400F field emission scanning electron microscope (Jeol, Japan) at an acceleration voltage of 5 kV.

2.4 Atomic force microscopy

Roughness of the investigated membranes (pre-wetted) was analyzed by Atomic Force Microscope III A (Digital Instruments Inc., Santa Barbara, CA). Point probe silicon cantilever tip was used in contact mode using Nanoscope III A software (version 5.12b15). The mean value of the surface roughness relative to the center plane R_a was calculated by the following equation $R_a = 1/L_x L_y \int_0^{L_y} \int_0^{L_x} [f(x, y)] dx dy$, where $f(x, y)$ is the surface relative to the center plane and L_x and L_y are the dimensions of the surface. The evaluation of the roughness parameters of each membranes sample was based on three scanned areas.

2.5 Contact angle

The surface properties of the membranes were characterized by contact angle (CA) measurements against distilled water using the captive bubble technique with a goniometer including a microscope (Zeiss, Germany). The receding (dewetting) and the advancing (wetting) CA were taken from three different places for each membrane.

2.6 Zeta potential

Streaming potential measurements were carried out as described previously [21] with an EKA Electro Kinetic Analyzer (Anton Paar KG, Graz, Austria). Briefly, a flat plate measuring cell with an electrolyte channel between sample surfaces (effective area— $2 \times (74 \times 15) \text{ mm}^2$ and an effective height of 0.3 mm) was used. Measurements were performed at $25.0 \pm 0.5^\circ\text{C}$ using aqueous KCl solution ($I = 5 \times 10^{-3} \text{ mol l}^{-1}$). Equimolar KOH and HCl solutions were used for an adjustment of pH value. The zeta potential was calculated taking into account the surface conductivity.

2.7 Quantification of surface carboxylic groups

The content of the generated carboxylic groups on the membrane surface was measured by binding of the fluorescent dye thionin acetate (THA) as described previously [22]. THA is a cationic dye that labels the carboxylic group (–COOH) by salt formation. After equilibration and subsequent washing, the fluorescent cation can be exchanged under acidic conditions and measured in solution. For conversion of salts into carboxylic groups the samples were incubated in 0.01 N HCl in water/ethanol 1:1 for 1 h. After washing with distilled water the samples (disks with 25 mm in diameter) were immersed into a solution of 10 mg/l THA in ethanol. The samples were shaken at room temperature (RT) for 12 h. After three short washes with ethanol the samples were immersed in exactly 10 ml 0.01 N HCl in water/ethanol 1:1 and shaken for 2 h at RT. The solution was measured spectrofluorometrically (LS50B fluorescence spectrometer Perkin Elmer, Beaconsfield, UK) at 620 nm (594 nm excitation) and compared with a standard curve of THA.

2.8 Blood collection and preparation

Platelet rich plasma (PRP) and platelet poor plasma (PPP) were obtained from fresh buffy coat. A CPD mixture (citrate:phosphate:dextrose) was used as anticoagulant. PRP was prepared by centrifugation of blood at $200 \times g$ for 10 min. The supernatant PRP was collected and the blood was centrifuged at $2,000 \times g$ for 20 min to prepare PPP. The platelet count in PRP was adjusted to 200,000/ μl by mixing PRP and PPP.

2.9 Platelet adhesion

PRP at a concentration of 200,000 platelets/ μl was added (600 μl /well) to membrane discs (13 mm in diameter) in 24 well plates. After 30 min contact time the supernatant PRP was collected, and the platelet count was measured

with a Coulter Counter, Type M II (Coulter Corp., Miami, FL, USA). Comparison of the platelet counts before and after membrane contact yielded the number of retained and adherent platelets, respectively.

2.10 Platelet adhesion and activation

Platelet adhesion and activation was assessed by immunostaining of the adherent platelets using antibodies against platelet glycoproteins (GPIb and GPIIIa). The cells were morphologically categorized by using the method of Grunkemeier et al. [23]. The morphologic categories are listed in Table 1. Immunofluorescence staining for GPIb and GPIIIa was carried out as followed. After 1 h contact of PRP with the membrane discs ($d = 13$ mm in diameter) at 37°C , samples were washed with phosphate buffer saline (PBS) pH 7.4, followed by a fixation with 3% paraformaldehyde and saturated with 1% bovine serum albumin (BSA) both in PBS. The labeling of the platelets was performed with a mouse monoclonal antibody CD42b (anti-GP Ib, Cymbus Biotechnology, Chandlers Ford SO53 4NF, UK) or mouse antibody anti-integrin β_3 (anti-GP IIIa, Chemicon International, Inc., Temecula, SA, USA) at a dilution of 1:100, followed by a 1:200 diluted polyclonal goat anti-mouse IgG antibody, Cy3TM-conjugated (Jackson Immuno Research Laboratories, West Grove, PA, USA).

After mounting the samples were examined by a Confocal Laser Scanning Microscope (CLSM 510, Zeiss, Göttingen, Germany).

2.11 Measurement of plasma kallikrein-like activity

The contact of blood with foreign surfaces causes the activation of coagulation cascade by the intrinsic pathway. It starts with activation of factor XII to XIIa through the conversion of plasma prekallikrein to kallikrein. The presence of kallikrein in the supernatant was measured spectrophotometrically by the chromogenic substrate S-2302 (Chromogenix/Haemochrom Diagnostica, Essen, Germany)

Table 1 Criteria used to categorize platelet morphology from Grunkemeier et al. [23]

Morphology	Description of platelet morphology
Round (R)	No pseudopodia present, platelet either round or discoid
Dendritic (D)	One or more pseudopodia present, but no flattening of platelets
Spread dendritic (SD)	One or more pseudopodia present, some flattening of platelet, little spreading of hyaloplasm between pseudopodia
Spreading (S)	Hyaloplasm partially spread between extended pseudopodia, or significant spreading of hyaloplasm between pseudopodia, but maximum diameter of platelet less than $7.5 \mu\text{m}$
Fully spread (FS)	Hyaloplasm extensively spread, no distinct pseudopodia, maximum platelet diameter of $7.5 \mu\text{m}$ or greater
Non-viable (NV)	Similar to fully spread morphology but with extensive fragmentation of the membrane, or platelet appears to have spread and subsequently retracted leaving a rounded up center with attached remnants of cellular material at previous sites of adhesion

using a method described previously [24]. Briefly, PPP (diluted 1:5 with Tris-HCl, pH 7.8) had contact with materials (13 mm membrane discs) in 24 well plates (1 ml PPP per well) for 30 min. In 96 well plates, 200 μ l of PPP was mixed with 100 μ l S-2302 (4 mM) and incubated at 37°C for up to 25 min. During this time, the reaction kinetics were tracked every 5 min at 405 vs. 620 nm (TECAN Spectra Fluor Plus plate reader, Crailsheim, Germany). The slope of the optical density kinetics gives a measure of the kallikrein-like activity.

2.12 Statistical analysis

All statistical computations were carried out with InStat[®] 3.00 software (GraphPad Software Inc., San Diego, USA). The values were considered significantly different if the *P*-value was <0.05.

3 Results

3.1 Material surface properties

Phase inversion process was used for the preparation of flat sheet membranes with low porosity from PEI. According to

the SEM micrographs (Fig. 1), the PEI membranes are characterized by a macrovoidal structure (Fig. 1b), typical for the applied preparation procedure. The active layer of the membrane (Fig. 1a) possesses a microporous structure with pore size in a range of 1–2 nm. The functionalization of PEI membrane with –COOH groups did not cause any significant differences in the structure of the active layer (Fig. 1c–d).

The roughness (*R*_a) of the PEI membranes measured by AFM showed only a slight rise in roughness with wet chemical treatment and did not reveal any significant changes in topography after the functionalization process (Table 2). The roughness of the three PEI membranes was in the range between 13 and 15 nm (25 × 25 μ m² scanned field). Only PET film (reference material) showed approximately three times smoother surface with a roughness of about 5.5 nm.

The amount of –COOH groups on the material surface was estimated by THA assay, which gave a value of about 4.6 nmol of carboxylic groups per cm² of membrane area for the unmodified PEI under the assumption that 1 mole of THA binds to 1 mole of carboxylic groups [22].

Within the first 10 min of the membrane modification with IDA the number of carboxylic groups raised and reached a plateau value of about 8.6 nmol/cm² indicating

Fig. 1 SEM micrographs of the membranes: (a) top view of the active surface layer of unmodified PEI; (b) cross-section of unmodified PEI; (c) top view of PEI modified with IDA for 1 min (PEI-1); (d) top view of PEI modified with IDA for 30 min (PEI-2)

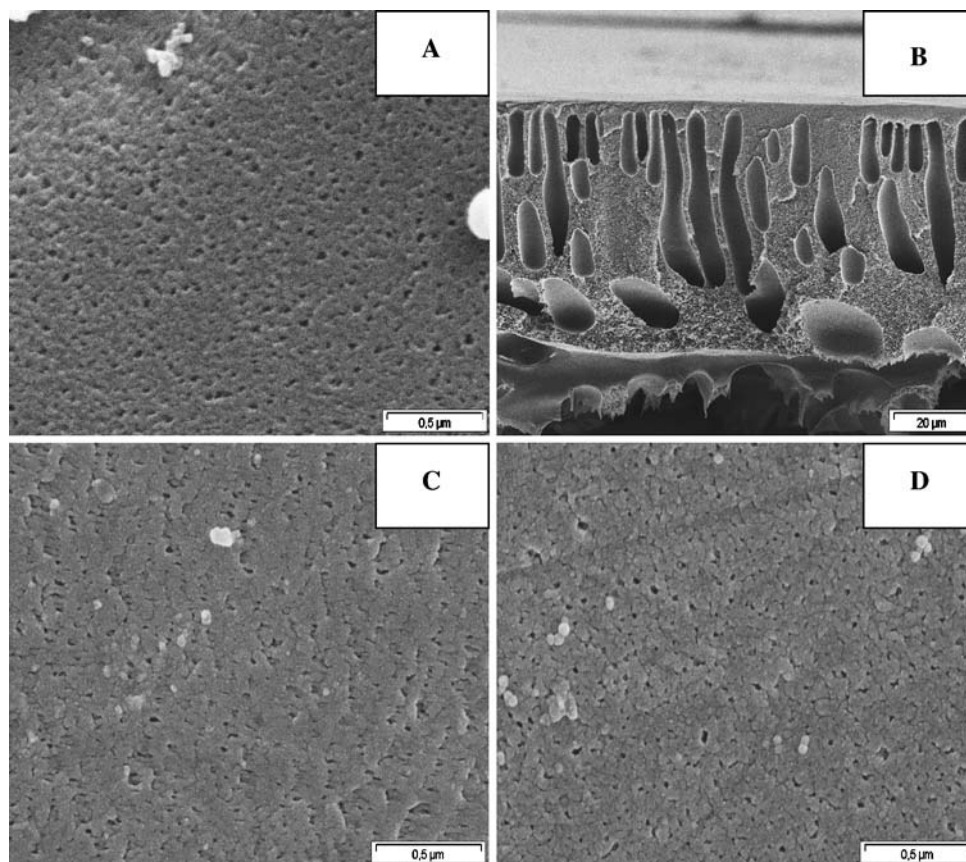


Table 2 Mean values of the surface roughness Ra

Surface	Average Ra (nm)	Standard deviation (nm)
PEI	13.5	5.2
PEI-1	15.3	4.3
PEI-2	15.3	2.5
PET	5.5	1.6

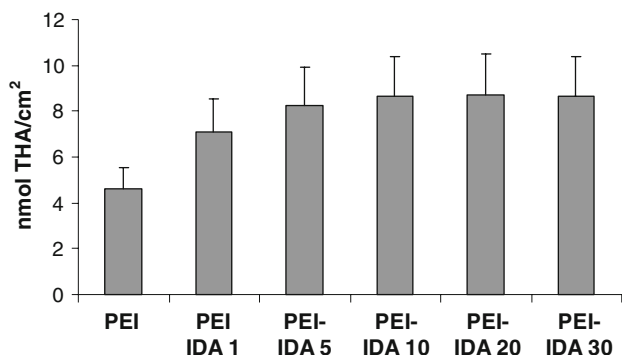


Fig. 2 Content of carboxylic groups on the surface of PEI membranes after treatment for 1 (PEI-IDA1 = PEI-1), 5 (PEI-IDA5), 10 (PEI-IDA10), 20 (PEI-IDA20), and 30 (PEI-IDA30 = PEI-2) min with sodium salt of iminodiacetic acid (IDA). The content of carboxylic groups was measured using THA assay

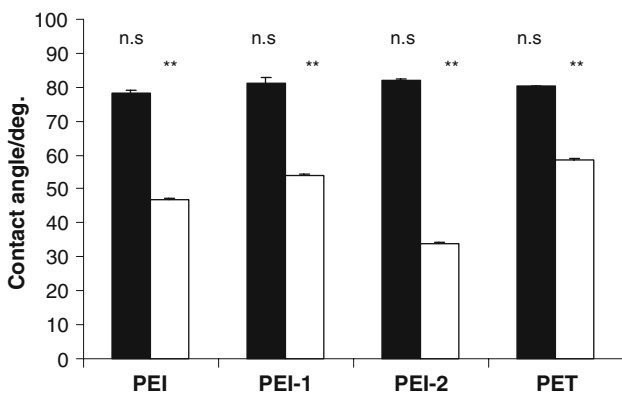


Fig. 3 Advancing (black columns) and receding (white columns) water captive bubble CA for PEI, PEI-1, PEI-2 and PET were measured at three different points on each membrane in quadruplicate. *t*-Test was used for statistical analysis. n.s., non-significant differences for advancing CA; (**), significant with $P < 0.05$ differences for receding CA

that about 4 nmol of carboxylic groups per cm² of membrane area were formed by IDA treatment (Fig. 2). For all further experiments, the membranes modified for 1 min (PEI-1) and 30 min (PEI-2) were used.

The water CA of the membranes is given in Fig. 3. Unmodified PEI showed an advancing CA of 78.1° and receding CA about 39.1°. Modification with IDA did not show significant differences in the measured advancing CA

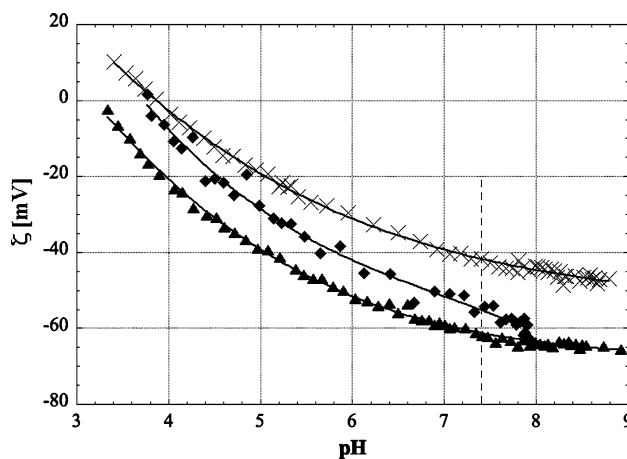


Fig. 4 Zeta potential of PEI (◆), PEI-2 (▲) and PET (×) membranes estimated by streaming potential measurements

of the PEI-1 and PEI-2 membranes. A difference was found only between receding CA's of the membranes. A significant decrease in the receding CA was found for PEI-2 (28.3°) corresponding to the increased amount of -COOH groups. The observed CA hysteresis (the difference between advancing and receding CA) for PEI-2 (54°) was almost twice higher compared to the other membranes.

Streaming potential measurements were performed only for unmodified PEI and PEI-2 (Fig. 4) with the assumption for an expected similarity between PEI-1 and PEI-2 on the basis of the -COOH content. The unmodified PEI membrane has an isoelectric point (IEP) at pH 3.7 and showed an increase of the magnitude of the negative zeta potential with the increasing of pH. At pH 7.4 (physiological pH) the streaming potential was about -55 mV. Prolonged treatment of PEI with IDA up to 30 min (PEI-2) resulted in a decrease of the IEP to pH 3.2 connected with a more negative streaming potential of -61 mV at pH 7.4. The reference PET membrane, which has an IEP at pH 3.9,

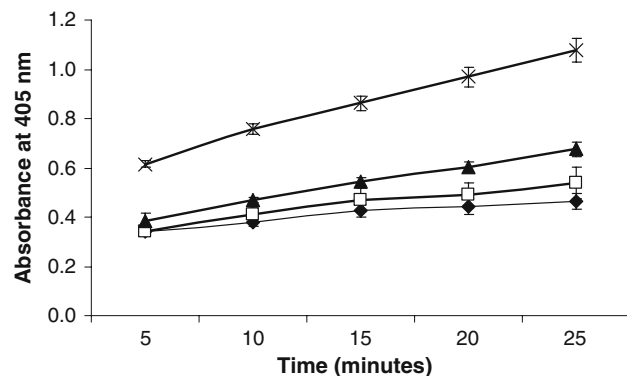


Fig. 5 Kallikrein-like activity of plasma after contact with PEI (◆), PEI-1 (□), PEI-2 (▲), and PET (×) polymers for 30 min detected by cleavage of a chromogenic substrate (S-2302) and measured spectrophotometrically at 405 nm. The graph represents absorbance versus cleaving time

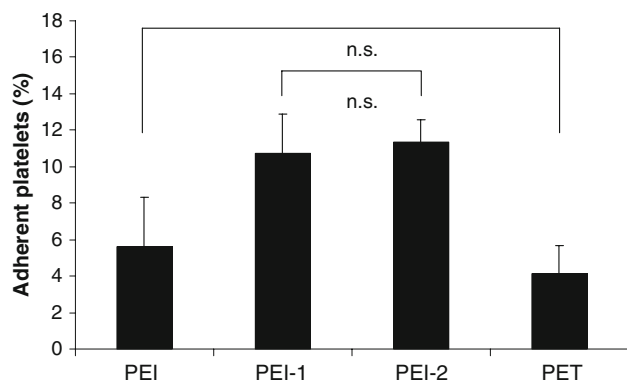


Fig. 6 Platelet adhesion on polymer membranes after contact with PRP for 30 min estimated by platelet retention (n.s., not significant)

showed the least negative zeta potential value of about -42 mV at physiological pH.

3.2 Plasma kallikrein assay

Plasma kallikrein was detected by cleavage of a specific substrate (S-2302, H-D-Pro-Phe-Arg-pNA.2HCl). Kallikrein-like activity was the lowest on unmodified PEI

Fig. 7 Adhesion of platelets to PEI (a), PEI-1 (b), PEI-2 (c), and PET (d). Adherent platelets were labeled with monoclonal antibody anti-GPIIIa followed by IgG Cy³-conjugated secondary antibody. Bar is 20 μ m

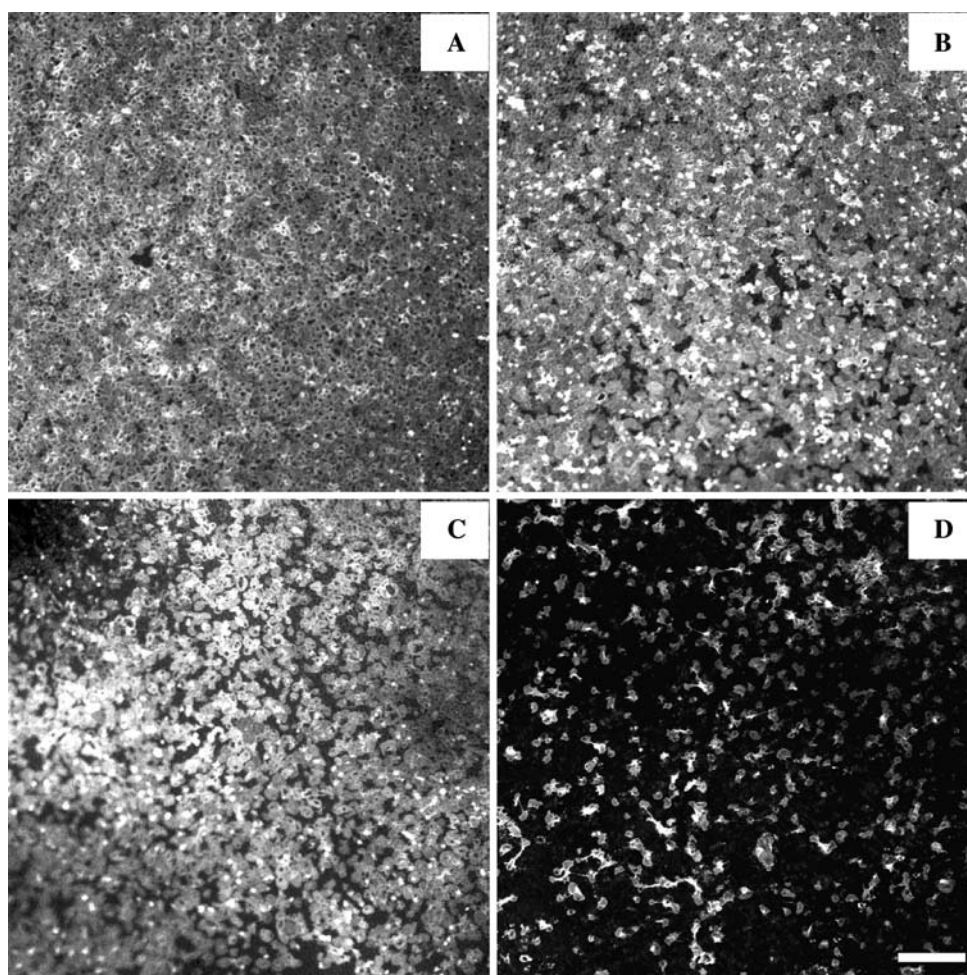


(Fig. 5). The functionalization of PEI with the larger amounts of $-\text{COOH}$ groups caused an enhanced kallikrein-like activity indicated by a higher slope of curve in Fig. 5. The highest kallikrein-like activity was found on PET.

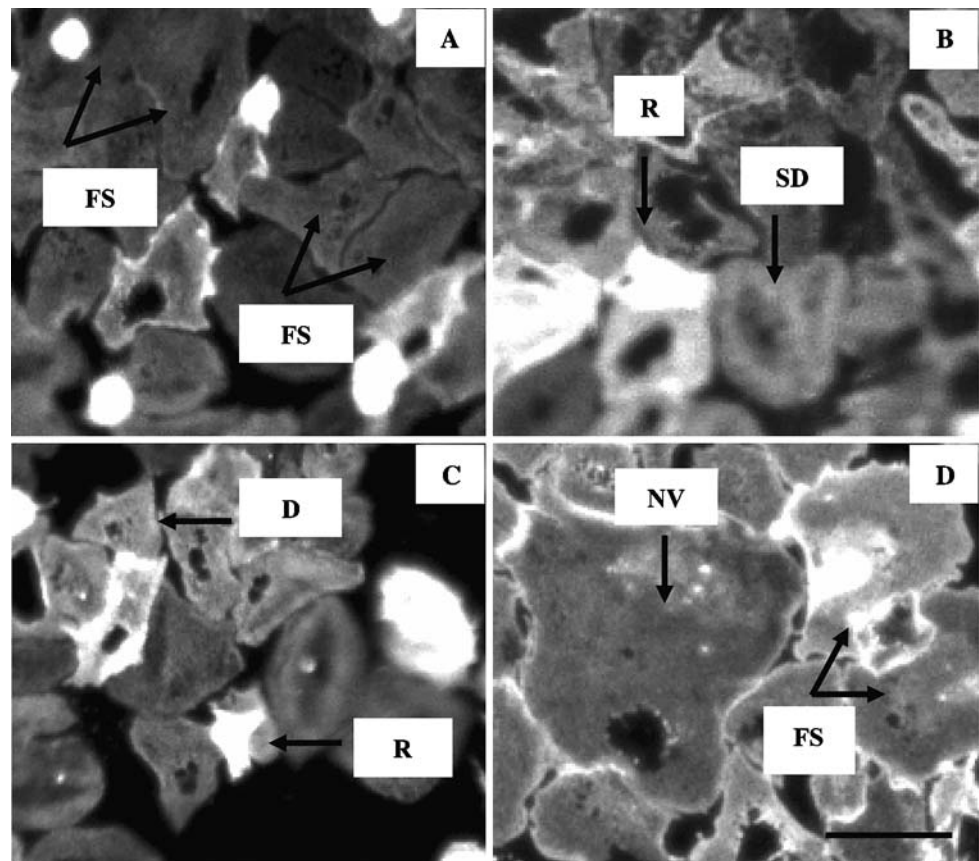
3.3 Platelet adhesion rate

The amount of adherent platelets on the polymer membranes was estimated by incubation of platelets on the investigated materials for 30 min and counting the remaining cells in supernatant. The difference in the cell number between t_0 (200,000 platelets/ μ l) and t_{30} gave the number of the adherent platelets in percentage (Fig. 6). The modification of PEI with $-\text{COOH}$ groups caused a higher amount of platelet adhesion. The rate of platelet adhesion on unmodified PEI was lower and comparable with the cell amount adhered on PET.

3.4 Platelet adhesion and activation

The adhesion and activation of platelets onto the examined polymers were investigated by immunofluorescence microscopy with a CLSM using antibodies against platelet

Fig. 8 Adhesion of platelets to PEI (a), PEI-1 (b), PEI-2 (c), and PET (d). Adherent platelets were labeled with monoclonal antibody anti-GPIb followed by IgG Cy³-conjugated secondary antibody. Bar is 5 μ m. Morphology: R, round; D, dendritic; SD, spread dendritic; FS, fully spread; and NV, non-viable. Bar is 5 μ m



glycoprotein GPIIIa and GPIb. The immunofluorescence micrographs in Figs. 7 and 8 represent the degree of platelet adhesion and activation on the investigated polymers. The enhanced platelet adhesion on PEI-1 and PEI-2 (observed by platelet counting in Fig. 6) was confirmed by the immunofluorescence experiments (Fig. 7b and c). Platelets adherent to the investigated surfaces were categorized into the morphological categories listed in Table 1. Representative micrographs for each material are shown in Fig. 8. Interestingly, nevertheless that PEI-1 and PEI-2 attracted higher amount of platelets, significant part of them was in relatively low activation state. On those materials, the platelet population exhibited cells with round (R) shape morphology without pseudopodia and a low amount of dendritic (D) or spread dendritic-type (SP) cells (Fig. 8b and c). In contrast, as can be seen from the micrograph (Fig. 7d), although the total amount of adhered platelets to PET was considerably low, the cells were fully spread (FS) or even some cells were non-viable (NV), which fact indicates for a high rate of activation (Fig. 8d).

4 Discussion

In this article, we developed two surface modifications of PEI material with carboxylic groups in order to study how

the material surface properties could influence hemocompatibility of these biomaterials used for blood-contacting medical devices. The results were compared with PET film, which is a widely used vascular graft material.

Surface modification was confirmed by measured increase in $-COOH$ group content and the enhanced negative surface charge (streaming potential measurements) of the modified membranes. However, there was no major shift in the advancing water contact angles of PEI surfaces after modification, which kept their hydrophobic nature. Changes were found for receding water contact angles, confirming increased heterogeneity of surface structures connected with the surface modification. That fact could be explained by the low surface coverage with $-COOH$ groups ($\leq 4 \text{ nmol/cm}^2$) or by the uncompleted process of the modification [2, 25].

The blood-contacting properties of the membranes were investigated by studying the activation of coagulation system and the adhesion/activation rate of platelets. It is well known that the activation of the coagulation system on non-physiological surfaces is initiated by the intrinsic pathway in which the kallikrein cascade plays an important role in thrombin generation, which mediates conversion of fibrinogen to fibrin [26]. By measuring the generated level of kallikrein in plasma after contact with the material surface it was found that, in general, PEI membranes

showed lower coagulation activations than PET. However the increased amount of acidic groups (–COOH) on the surface of PEI-2 compared to PEI provoked a higher activation. This is in accordance with the results of Sperling et al. [3] studying the self assembled monolayer (SAM) surfaces of alkanethiols with various terminating groups (–OH, –CH₃, and –COOH) and binary mixtures of them, and the common understanding and findings that negatively charged surfaces induce zymogen activation in vitro [3, 27]. In addition, Vogler and coworkers [28–30] studying the activation of coagulation cascade showed that the increased electrostatic interactions between proteins and the (charged) surfaces upon adsorption maintain the biological function of the coagulation enzymes by “non-denaturation” mechanism. In this direction, also the investigations of Monien and coworkers [18] indicate a low affinity of carboxylic-based polymers [such as poly(acrylic acid)] for antithrombin which might lower the anticoagulant activity of the polymer surface. The higher rate of kallikrein production activated by contact with modified PEI (Fig. 5) leading to fibrin generation was most probably the reason for the higher extent of platelet adhesion onto carboxylated PEI membranes compared to plain PEI, as is shown on Fig. 7. Our data are in contradiction with the results of Sperling et al. [3] who did not find a correlation between coagulation and platelet adhesion for any of the investigated SAM's.

However, interesting behavior showed PET material. Although platelets did not adhere to a high extent on PET, they showed quite different cell morphology. Since the predominant platelet morphology on PEI membranes was discoid and only few spherical shaped platelets with pseudopodia were detected, on PET the highest contact activation (Fig. 5) was connected with fully spread platelets (even non-viable cells) confirming the high rate of platelet activation (Fig. 8).

However, the functionalization of PEI membrane with carboxylic groups did not meet the expectation for improved hemocompatibility. In the literature there are also inconsistent results for using carboxylic groups to improve the blood compatibility. For instance some investigators have revealed that dextrans, which contained only carboxylic groups, are inactive in their anticoagulant property [31]. Even Ito et al. [32] have shown that the incorporation of –COOH groups into the polymer reduced heparin-like activity contrary to the results of Jozefowicz et al. [7].

As a result of the present investigation, it was found that PEI (non-modified and non-carboxylated) is a material with higher hemocompatibility (in terms of coagulation and platelet adhesion/activation) than PET membrane but at the same time, the combination of the high amount of platelet adhesion and kallikrein production makes those

surfaces still with a high potential risk for thrombus formation. Based on the present results we could speculate on the need to retain sulfate groups on the polymer surface for better heparin substitutes and better hemocompatibility. The results of this rational design strategy will be reported in the future.

References

1. Z. Kim, K. Park, D. Han, *Encyclopedia of polymeric materials* (Salamone JC, Chicago, 1998), p. 825
2. B. Seifert, G. Mihanetzis, T. Groth, W. Albrecht, K. Richau, Y. Missirlis, D. Paul, G. Von Sengbusch, *Artif. Organs* **26**, 189 (2002)
3. C. Sperling, R. Schweiss, U. Streller, C. Werner, *Biomaterials* **26**, 6547 (2005)
4. N. Faucheux, R. Schweiss, K. Lützow, C. Werner, T. Groth, *Biomaterials* **25**, 2721 (2004)
5. A. Biebricher, A. Paul, P. Tinnefeld, A. Golzhauser, M. Sauer, *J. Biotechnol.* **112**, 97 (2004)
6. B. Casu, *Ann. N. Y. Acad. Sci.* **556**, 1 (1989)
7. M. Jozefowicz, J. Jozefonvicz, *Pure Appl. Chem.* **56**, 1335 (1984)
8. H. Kawakami, Y. Mori, J. Takagi, S. Nagaoka, T. Kanamori, T. Shinbo, S. Kubota, *ASAIO J.* **43**, M490 (1997)
9. T. Stieglitz, J.U. Meyer, *Med. Device Technol.* **10**, 28 (1999)
10. Y. Imai, A. Watanabe, E. Masuhara, Y. Imai, *J. Biomed. Mater. Res.* **17**, 905 (1983)
11. R.R. Richardson Jr., J.A. Miller, W.M. Reichert, *Biomaterials* **14**, 627 (1993)
12. O. Petillo, G. Peluso, L. Ambrosio, L. Nicolais, W.J. Kao, J.M. Anderson, *J. Biomed. Mater. Res.* **28**, 635 (1994)
13. R. Tzoneva, T. Groth, G. Altankov, D. Paul, *J. Mater. Sci. Mater. Med.* **13**, 1235 (2002)
14. A. Cardon, S. Aillet, J.F. Desjardins, V. Hocdet, R. Tardivel, J. Le Du, F. Langlais, Y. Kerdiles, B. Saiag, *J. Mal. Vasc.* **24**, 118 (1999)
15. K. Kneifel, K.V. Peinemann, *J. Memb. Sci.* **65**, 295 (1992)
16. W. Albrecht, B. Seifert, T. Weigel, M. Schossig, A. Hollander, T. Groth, R. Hilke, *Macromol. Chem. Phys.* **204**, 510 (2003)
17. F. Meng, G.H. Engbers, A. Gessner, R.H. Muller, J. Feijen, *J. Biomed. Mater. Res.* **70A**, 97 (2004)
18. B. Monien, K. Cheang, U. Desai, *J. Med. Chem.* **48**, 5360 (2005)
19. B. Monien, U. Desai, *J. Med. Chem.* **48**, 1269 (2005)
20. R. Tzoneva, M. Heuchel, T. Groth, G. Altankov, W. Albrecht, D. Paul, *J. Biomater. Sci. Polym. Ed.* **13**, 1033 (2002)
21. K. Richau, R. Mohr, V. Kudela, J. Schauer, *J. Ion. Exch.* **14**, 201 (2003)
22. V.B. Ivanov, J. Behnisch, A. Hollander, F. Mehdorn, H. Zimmermann, *Surf. Interface Anal.* **24**, 257 (1996)
23. J.M. Grunkemeier, W.B. Tsai, T.A. Horbett, *J. Biomater. Sci. Polym. Ed.* **12**, 1 (2001)
24. T. Groth, J. Synowitz, G. Malsch, K. Richau, W. Albrecht, K.P. Lange, D. Paul, *J. Biomater. Sci. Polym. Ed.* **8**, 797 (1997)
25. J. Vienken, M. Diamantoglou, C. Hahn, H. Kamusewitz, D. Paul, *Artif. Organs* **19**, 398 (1995)
26. T. Matsuda, *Nephrol. Dial. Transplant.* **4**(Suppl), 60 (1989)
27. A.H. Schmaier, *Thromb. Haemost.* **77**, 101 (1997)
28. E. Vogler, J. Graper, G. Harper, H. Sugg, L. Lander, W. Brittain, *J. Biomed. Mater. Res.* **29**, 1005 (1995)
29. E. Vogler, J. Graper, H. Sugg, L. Lander, W. Brittain, *J. Biomed. Mater. Res.* **29**, 1017 (1995)
30. E. Vogler, J. Nadeau, J. Graper, *J. Biomed. Mater. Res.* **40**, 92 (1998)
31. M. Mauzac, N. Aubert, J. Jozefowicz, *Biomaterials* **3**, 221 (1982)
32. Y. Ito, Y. Iguchi, T. Kashiwagi, Y. Imanishi, *J. Biomed. Mater. Res.* **25**, 1347 (1991)